Two-gluon and trigluon glueballs from dynamical holography QCD *

Yi-dian Chen(陈亦点)[1;1)] Mei Huang(黄梅)[1,2;2)]

[1] Institute of High Energy Physics, Chinese Academy of Sciences, Beijing 100049, China
[2] Theoretical Physics Center for Science Facilities, Chinese Academy of Sciences, Beijing 100049, China

Abstract: We study the scalar, vector and tensor two-gluon and trigluon glueball spectra in the framework of the 5-dimension dynamical holographic QCD model, where the metric structure is deformed self-consistently by the dilaton field. For comparison, the glueball spectra are also calculated in the hard-wall and soft-wall holographic QCD models. In order to distinguish glueballs with even and odd parities, we introduce a positive and negative coupling between the dilaton field and glueballs, and for higher spin glueballs, we introduce a deformed 5-dimension mass. With this set-up, there is only one free parameter from the quadratic dilaton profile in the dynamical holographic QCD model, which is fixed by the scalar glueball spectra. It is found that the two-gluon glueball spectra produced in the dynamical holographic QCD model are in good agreement with lattice data. Among six trigluon glueballs, the produced masses for $1^{\pm-}$ and 2^{--} are in good agreement with lattice data, and the produced masses for 0^{--}, 0^{+-} and 2^{+-} are around 1.5 GeV lighter than lattice results. This result might indicate that the three trigluon glueballs of 0^{--}, 0^{+-} and 2^{+-} are dominated by the three-gluon condensate contribution.

Keywords: glueball, holographic QCD model, AdS/CFT correspondence

PACS: 11.25.Tq **DOI:** 10.1088/1674-1137/40/12/123101

1 Introduction

Quantum chromodynamics (QCD) is accepted as the fundamental theory of describing the strong interaction. In the high energy regime, QCD has the property of asymptotic freedom, and perturbative QCD calculations have been tested with high precision. However, in the low energy regime, the nonperturbative aspect related to QCD vacuum properties and hadron spectra remains as an outstanding challenge. The non-Abelian feature of QCD makes it possible to form bound states of gauge bosons, i.e. glueballs (gg, ggg, etc.) [1]. The gauge field plays a more important dynamical role in glueballs than that in the standard hadrons, therefore studying particles like glueballs offers a good opportunity to understand the nonperturbative aspects of QCD.

The glueball spectrum has attracted much attention for more than three decades [1], and it has been widely investigated by using various non-perturbative methods. For example, from first principles calculation by using lattice QCD [2–6], by using flux tube model [7] as well as by using QCD sum rules [8–10]. For more information, please refer to review papers [11].

The discovery of gravity/gauge duality, or anti-de Sitter/conformal field theory (AdS/CFT) correspondence [12–14], offers a new possibility to tackle the difficulty of strongly coupled gauge theories. For reviews see Ref. [15]. In recent decades, many efforts have been invested from both top-down and bottom-up approaches in examining nonperturbative QCD properties, e.g., QCD equation of state, phase transitions, fluid properties of quark-gluon plasma [16], meson spectra [17–19], and baryon spectra [20], as well as in the glueball sector [21–25]. It is expected that the holography approach can shed some light on our understanding of the nonperturbative aspects of QCD.

QCD is a non-conformal gauge theory, and the Sakai-Sugimoto (SS) model [26] is one of the most successful non-conformal top-down holographic QCD models. The glueball spectra in the Sakai-Sugimoto model have been investigated in the literature, see Ref. [27]. Glueballs have also been widely studied by using the bottom-up approach [23], where most studies are based on hard-wall [17] and soft-wall holographic QCD models [18] with the

Received 23 January 2016, Revised 3 September 2016

∗ Supported by the NSFC (11175251, 11621131001), DFG and NSFC (CRC 110), CAS Key Project KJCX2-EW-N01, K.C.Wong Education Foundation, and Youth Innovation Promotion Association of CAS

1) E-mail: chenyd@ihep.ac.cn

2) E-mail: huangm@ihep.ac.cn

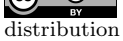

conformal AdS_5 background metric.

A successful holographic QCD model should grasp two main features of nonperturbative QCD properties: spontaneous chiral symmetry breaking and color charge confinement. The dynamical holographic QCD model (DhQCD), which can describe both chiral symmetry breaking and confinement, has been constructed in Ref. [28–30]. In this model, the gluon dynamics background is determined by the coupling between the graviton and the dilaton field $\Phi(z)$, which is responsible for the gluon condensate and confinement, and the scalar field $X(z)$ is introduced to mimic chiral dynamics. Evolution of the dilaton field and scalar field in 5D resemble the renormalization group from ultraviolet (UV) to infrared (IR). This DhQCD model describes the scalar glueball spectra and the light meson spectral quite well [28–30]. Further studies [31, 32, 42] show that this DhQCD model can also describe the QCD phase transition, the equation of state of QCD matter, and temperature dependent transport properties, including shear viscosity, bulk viscosity, electric conductivity as well as the jet quenching parameter.

For the scalar glueball spectra, it was shown in Ref.[29] that, comparing with the results in the hard-wall and soft-wall holographic QCD models [23], the scalar glueballs, including the lowest state and excited states, can be surprisingly well described in the DhQCD model. However, the scalar glueball 0^{++} has the same quantum number as the scalar quarkonium $\bar{q}q$ and tetraquark $\bar{q}q\bar{q}q$ [34] states, and the complexity of determining the glueball states lies in that gluonic bound states might always mix with $\bar{q}q$ and $\bar{q}q\bar{q}q$ states. For example, one has to distinguish the lightest scalar glueball state among 19 scalar mesons observed in the energy range below 2 GeV [35, 36]. Therefore, it is interesting to investigate odd glueballs with unconventional quantum numbers which cannot be carried by quark-antiquark bound states. These include $J^{PC}=0^{--},0^{+-},2^{+-},3^{-+}$ glueballs, which can only be made of at least three-gluon bound states.

This motivates us to investigate the whole glueball spectra including (scalar, vector as well as tensor glueballs and their excitations) in the framework of the DhQCD model. The paper is organized as follows. In Section 2 we give the operators of two-gluon and trigluon glueballs. We introduce the dynamical soft-wall holographic QCD model in Section 3, and calculate the glueball spectra in the dynamical holographic QCD model in Section 4. It is found that higher-spin glueballs are very heavy compared with lattice data, and the even and odd parities cannot be distinguished. Therefore, we introduce a deformed 5-dimension mass for higher spin glueballs, and in order to distinguish glueballs with even and odd parities, we introduce the positive and negative coupling between the dilaton field and glueballs. With this set-up, we calculate the glueball spectra in the modified dynamical holographic QCD model in Section 5 and find that the two-gluon glueball spectra are in good agreement with lattice data and the trigluon glueball spectra agree with results from QCD sum rules. Finally, a short summary is given in Section 6.

2 Two-gluon and trigluon glueballs

The AdS/CFT correspondence establishes a one-to-one correspondence between a certain class of 4D local operators in the $\mathcal{N}=4$ superconformal gauge theory and 5D supergravity fields representing the holographic correspondents in the $AdS_5\times S^5$ bulk theory. According to the AdS/CFT dictionary, the conformal dimension of a (f-form) operator on the ultraviolet (UV) boundary is related to the M_5^2 of its dual field in the bulk as follows [12–14]:

$$M_5^2=(\Delta-f)(\Delta+f-4)\,. \tag{1}$$

In the bottom-up approach, for example in the holographic QCD models, one can expect a more general correspondence, i.e. each operator $\mathcal{O}(x)$ in the 4D field theory corresponds to a field $O(x,z)$ in the 5D bulk theory. To investigate the glueball spectra, we consider the lowest dimension operators with the corresponding quantum numbers and defined in the field theory living on the 4D boundary. We show the two-gluon and trigluon glueball operators and their corresponding 5D masses in Table 1.

Table 1. 5D mass square of two-gluon and trigluon glueballs. The operators are taken from [22] and [9, 10].

J^{PC}	4D : $\mathcal{O}(x)$	Δ	f	M_5^2
0^{++}	$\mathrm{Tr}(G^2)$	4	0	0
0^{--}	$\mathrm{Tr}(\tilde{G}\{D_{\mu_1}D_{\mu_2}G,G\})$	8	0	32
0^{-+}	$\mathrm{Tr}(G\tilde{G})$	4	0	0
$1^{\pm-}$	$\mathrm{Tr}(G\{G,G\})$	6	1	15
2^{++}	$\mathrm{Tr}\left(G_{\mu\alpha}G_{\alpha\nu}-\frac{1}{4}\delta_{\mu\nu}G^2\right)$	4	2	4
2^{++}	$E_i^aE_j^a-B_i^aB_j^a-\mathrm{trace}$	4	2	4
2^{-+}	$E_i^aB_j^a+B_i^aE_j^a-\mathrm{trace}$	4	2	4
$2^{\pm-}$	$\mathrm{Tr}(G\{G,G\})$	6	2	16

For a trigluon glueball 0^{--}, the detailed structure of the operator is given in Ref. [9]

$$j^A_{0^{--}}\sim d^{abc}[g^t_{\alpha\beta}\tilde{G}^a_{\mu\nu}][\partial_\alpha\partial_\beta G^b_{\nu\rho}][G^c_{\rho\mu}], \tag{2}$$

$$j^B_{0^{--}}\sim d^{abc}[g^t_{\alpha\beta}G^a_{\mu\nu}][\partial_\alpha\partial_\beta \tilde{G}^b_{\nu\rho}][G^c_{\rho\mu}], \tag{3}$$

$$j^C_{0^{--}}\sim d^{abc}[g^t_{\alpha\beta}G^a_{\mu\nu}][\partial_\alpha\partial_\beta G^b_{\nu\rho}][\tilde{G}^c_{\rho\mu}], \tag{4}$$

$$j^D_{0^{--}}\sim d^{abc}[g^t_{\alpha\beta}\tilde{G}^a_{\mu\nu}][\partial_\alpha\partial_\beta \tilde{G}^b_{\nu\rho}][\tilde{G}^c_{\rho\mu}], \tag{5}$$

where d^{abc} stands for the totally symmetric $SU_c(3)$ structure constant and $g^t_{\alpha\beta}=g_{\alpha\beta}-\partial_\alpha\partial_\beta/\partial^2$.

The interpolating currents of the 2^{+-} oddball 2^{+-} take the form as [10],

$$j^{2^{+-},A}_{\mu\alpha}(x)=g_s^3 d^{abc}[G^a_{\mu\nu}(x)][G^b_{\nu\rho}(x)][G^c_{\rho\alpha}(x)], \quad (6)$$

$$j^{2^{+-},B}_{\mu\alpha}(x)=g_s^3 d^{abc}[G^a_{\mu\nu}(x)][\tilde{G}^b_{\nu\rho}(x)][\tilde{G}^c_{\rho\alpha}(x)], \quad (7)$$

$$j^{2^{+-},C}_{\mu\alpha}(x)=g_s^3 d^{abc}[\tilde{G}^a_{\mu\nu}(x)][G^b_{\nu\rho}(x)][\tilde{G}^c_{\rho\alpha}(x)], \quad (8)$$

$$j^{2^{+-},D}_{\mu\alpha}(x)=g_s^3 d^{abc}[\tilde{G}^a_{\mu\nu}(x)][\tilde{G}^b_{\nu\rho}(x)][G^c_{\rho\alpha}(x)]. \quad (9)$$

3 The dynamical soft-wall holographic QCD model and gluodynamics

The dynamical soft-wall holographic QCD model is described in Ref. [29]. The pure gluon part of QCD can be modelled by the 5D graviton-dilaton coupled action:

$$S_G=\frac{1}{16\pi G_5}\int \mathrm{d}^5x\sqrt{g_s}\mathrm{e}^{-2\Phi} \left(R_s+4\partial_M\Phi\partial^M\Phi-V^s_G(\Phi)\right), \quad (10)$$

where G_5 is the 5D Newton constant, g_s, Φ and V^s_G are the 5D metric, the dilaton field and dilaton potential in the string frame, respectively. The metric is chosen to be

$$g^s_{MN}=b_s^2(z)(\mathrm{d}z^2+\eta_{\mu\nu}\mathrm{d}x^\mu\mathrm{d}x^\nu), \quad b_s(z)\equiv\mathrm{e}^{A_s(z)}. \quad (11)$$

Under the conformal transformation

$$g^E_{MN}=g^s_{MN}\mathrm{e}^{-4\Phi/3}, \quad V^E_G=\mathrm{e}^{4\Phi/3}V^s_G, \quad (12)$$

Eq.(10) can be rewritten in the Einstein frame

$$S^E_G=\frac{1}{16\pi G_5}\int \mathrm{d}^5x\sqrt{g_E} \left(R_E-\frac{4}{3}\partial_M\Phi\partial^M\Phi-V^E_G(\Phi)\right). \quad (13)$$

The Einstein equations are

$$E_{MN}+\frac{1}{2}g^E_{MN}\left(\frac{4}{3}\partial_L\Phi\partial^L\Phi+V^E_G(\Phi)\right) -\frac{4}{3}\partial_M\Phi\partial_N\Phi=0, \quad (14)$$

$$\frac{8}{3\sqrt{g_E}}\partial_M(\sqrt{g_E}\partial^M\Phi)-\partial_\Phi V^E_G(\Phi)=0. \quad (15)$$

Substituting the metric of Eq.(11) into the above equations, we can obtain:

$$-A^{''}_E+A^{'2}_E-\frac{4}{9}\Phi^{'2}=0, \quad (16)$$

$$\Phi^{''}+3A^{'}_E\Phi^{'}-\frac{3}{8}e^{2A_E}\partial_\Phi V^E_G(\Phi)=0, \quad (17)$$

where

$$b_E(z)=b_s(z)\mathrm{e}^{-\frac{2}{3}\Phi(z)}=\mathrm{e}^{A_E(z)}, \quad A_E(z)=A_s(z)-\frac{2}{3}\Phi(z). \quad (18)$$

In the string frame, the above two equations of motion are

$$-A^{''}_s-\frac{4}{3}\Phi^{'}A^{'}_s+A^{'2}_s+\frac{2}{3}\Phi^{''}=0, \quad (19)$$

$$\Phi^{''}+(3A^{'}_s-2\Phi^{'})\Phi^{'}-\frac{3}{8}\mathrm{e}^{2A_s-\frac{4}{3}\Phi}\partial_\Phi(\mathrm{e}^{\frac{4}{3}\Phi}V^s_G(\Phi))=0. \quad (20)$$

We take the same dilaton field as that in the KKSS model or soft-wall holographic QCD model [18], i.e.,

$$\Phi=\mu^2_G z^2. \quad (21)$$

It is simple to solve the metric A_E and the dilaton potential $V^E_G(\Phi)$ in the quadratic dilaton background

$$A_E(z)=\log\left(\frac{L}{z}\right)-\log\left({}_0F_1\left(5/4,\frac{\Phi^2}{9}\right)\right), \quad (22)$$

$$V^E_G(\Phi)=-\frac{12\,{}_0F_1\left(1/4,\frac{\Phi^2}{9}\right)^2}{L^2}+\frac{16\,{}_0F_1\left(5/4,\frac{\Phi^2}{9}\right)^2\Phi^2}{3L^2}, \quad (23)$$

with ${}_0F_1(a;z)$ the hypergeometric function.

4 Glueball spectra in the dynamical soft-wall holographic QCD model

4.1 Scalar glueballs

The 5D action for the scalar glueball $\mathscr{G}(x,z)$ in the string frame takes the same form as that in the original soft-wall model [24, 25]

$$S_{\mathscr{G}}=-\int \mathrm{d}^5x\sqrt{g_s}\frac{1}{2}\mathrm{e}^{-\Phi}\left[\partial_M\mathscr{G}\partial^M\mathscr{G}+M^2_{\mathscr{G},5}\mathscr{G}^2\right]. \quad (24)$$

The metric structure in the dynamical soft-wall model is solved from Eq. (17) instead of AdS_5.

The equation of motion for the scalar glueballs $\mathscr{G}$ is given below as

$$-\mathrm{e}^{-(3A_s-\Phi)}\partial_z(\mathrm{e}^{3A_s-\Phi}\partial_z\mathscr{G}_n)+\mathrm{e}^{2A_s}M^2_{\mathscr{G},5}\mathscr{G}_n=m^2_{\mathscr{G},n}\mathscr{G}_n. \quad (25)$$

Via the substitution $\mathscr{G}_n\to\mathrm{e}^{-\frac{1}{2}(3A_s-\Phi)}\mathscr{G}_n$, the equation can be brought into the Schroedinger-like equation

$$-\mathscr{G}^{''}_n+V_{\mathscr{G}}\mathscr{G}_n=m^2_{\mathscr{G},n}\mathscr{G}_n, \quad (26)$$

with the 5D effective Schroedinger potential

$$V_{\mathscr{G}}=\frac{3A^{''}_s-\Phi^{''}}{2}+\frac{(3A^{'}_s-\Phi^{'})^2}{4}+\mathrm{e}^{2A_s}M^2_{\mathscr{G},5}. \quad (27)$$

4.2 Vector glueballs

For vector glueballs $\mathscr{V}$, the 5D action is

$$S_V = -\int \mathrm{d}^5x\sqrt{g}\mathrm{e}^{-\Phi}\left(\frac{1}{4}F^{MN}F_{MN}+\frac{1}{2}M^2_{\mathscr{V},5}\mathscr{V}^2\right), \quad (28)$$

where $F_{MN}=\partial_M\mathscr{V}_N-\partial_N\mathscr{V}_M$.

The equation of motion for vector glueballs $\mathscr{V}$ is

$$-\mathrm{e}^{-(A_s-\Phi)}\partial_z(\mathrm{e}^{A_s-\Phi}\partial_z\mathscr{V}_n)+\mathrm{e}^{2A_s}M^2_{\mathscr{V},5}\mathscr{V}_n=m^2_{\mathscr{V},n}\mathscr{V}_n. \quad (29)$$

Via the substitution $\mathscr{V}_n\to\mathrm{e}^{-\frac{1}{2}(A_s-\Phi)}\mathscr{V}_n$, the equation can be brought into the Schroedinger-like equation

$$-\mathscr{V}_n^{''}+V_{\mathscr{V}}\mathscr{V}_n=m^2_{\mathscr{V},n}\mathscr{V}_n, \quad (30)$$

with the 5D effective Schroedinger potential

$$V_{\mathscr{V}}=\frac{A_s^{''}-\Phi^{''}}{2}+\frac{(A_s^{'}-\Phi^{'})^2}{4}+e^{2A_s}M^2_{\mathscr{V},5}. \quad (31)$$

4.3 Tensor glueballs

For tensor glueballs, the 5D action is

$$\begin{aligned}S_T=-\frac{1}{2}\int \mathrm{d}^5x\sqrt{g}\mathrm{e}^{-\Phi}(&\nabla_L h_{MN}\nabla^L h^{MN}\\&-2\nabla_L h^{LM}\nabla^N h_{NM}+2\nabla_M h^{MN}\nabla_N h\\&-\nabla_M h\nabla^M h+M^2_{h,5}(h^{MN}h_{MN}-h^2)),\end{aligned} \quad (32)$$

where $h=g^{MN}h_{MN}$. With the constraint

$$\nabla_M h^{MN}=0,\quad h=0,\quad h_{\mu\nu}=e^{2A_s}\mathscr{H}_{\mu\nu},\quad h_{Mz}=0, \quad (33)$$

The equation of motion for tensor glueballs $\mathscr{H}_{\mu\nu}$ is

$$\begin{aligned}&-\mathrm{e}^{-(3A_s-\Phi)}\partial_z(\mathrm{e}^{3A_s-\Phi}\partial_z\mathscr{H}_n)\\&+\mathrm{e}^{2A_s}M^2_{\mathscr{H},5}\mathscr{H}_n=m^2_{\mathscr{H},n}\mathscr{H}_n.\end{aligned} \quad (34)$$

Via the substitution $\mathscr{H}_n\to\mathrm{e}^{-\frac{1}{2}(3A_s-\Phi)}\mathscr{H}_n$, the equation can be brought into the Schroedinger-like equation

$$-\mathscr{H}_n^{''}+V_{\mathscr{H}}\mathscr{H}_n=m^2_{\mathscr{H},n}\mathscr{H}_n, \quad (35)$$

with the 5D effective Schroedinger potential

$$V_{\mathscr{H}}=\frac{3A_s^{''}-\Phi^{''}}{2}+\frac{(3A_s^{'}-\Phi^{'})^2}{4}+\mathrm{e}^{2A_s}M^2_{\mathscr{H},5}. \quad (36)$$

4.4 Numerical results

For numerical calculations, we have to fix parameters in the model. In the dynamical holographic model, there is only one free parameter, i.e., μ_G. We fix this parameter by fitting the scalar glueball spectra from lattice results [2–5] as shown in Table 2. The lattice data in Table 2 indicates the slope of the Regge spectra is around 4 GeV^2, which is equivalent to $\mu_G\simeq 1$ GeV in the dynamical holographic QCD model.

Table 2. Lattice data for 0^{++} glueball in unit of MeV. Lat1 data from Ref. [4], Lat2 and Lat3 data from Ref. [3], Lat4 [2] and Lat5 [5] are anisotropic results.

$n(0^{++})$	Lat1	Lat2	Lat3	Lat4	Lat5
	$N_c=3$	$N_c=3$	$N_c\to\infty$	$N_c=3$	$N_c=3$
1	1475(30)(65)	1580(11)	1480(07)	1730(50)(80)	1710(50)(80)
2	2755(70)(120)	2750(35)	2830(22)	2670(180)(130)	
3	3370(100)(150)				
4	3990(210)(180)				

We will also compare our results in the dynamical holographic QCD model with those in the hard-wall and soft-wall holographic QCD models. In the hard-wall holographic QCD model, the equation of motion for glueball $\mathscr{G}$ is:

$$-\mathrm{e}^{-cA_s}\partial_z(\mathrm{e}^{cA_s}\partial_z\mathscr{G}_n)+\mathrm{e}^{2A_s}M^2_{\mathscr{G},5}\mathscr{G}_n=m^2_{\mathscr{G},n}\mathscr{G}_n, \quad (37)$$

where $c=1$ for vector glueballs and $c=3$ for scalar and tensor glueballs. With the UV boundary condition $\mathscr{G}_n(\epsilon)=0$, the solution is:

$$\mathscr{G}_n(z)=z^{\frac{1+c}{2}}J_n(m_{\mathscr{G},n},z), \quad (38)$$

where $n=\sqrt{1+2c+c^2+4M^2_{\mathscr{G},5}}/2$ and J is a Bessel function. The IR boundary condition $\partial_z\mathscr{G}_n(z_m)=0$ gives the discrete spectrum of the glueballs. Here z_m is the hard cut-off, which is the only parameter in the hard-wall model, and can be fixed by the ground state of the scalar glueball 0^{++}. When we take the mass for the lowest scalar glueball as 1730 MeV, which fixes $z_m=452$ MeV in the hard wall model.

In the soft-wall model, where the dilaton background takes the quadratic form $\Phi=\mu_G^2z^2$ and the metric structure is still AdS$_5$, the Regge spectra for glueballs can be derived as [24, 25]

$$m_n^2=\mu_G^2\left\{4n+c+1+\sqrt{(c+1)^2+4M_5^2}\right\},\ n=0,1,2,\cdots \quad (39)$$

where $c=3$ in the case of scalars and tensors and $c=1$ in the case of vectors. There is also only one parameter

μ_G in the soft-wall model. The Regge slope of the 0^{++} glueball gives $\mu_G = 1$ GeV (SW†), and the lowest scalar glueball mass 1730 MeV gives $\mu_G = 0.5$ GeV (SW‡).

Table 3 shows the scalar glueball spectra in the dynamical soft-wall holographic QCD model, and the results are compared with combined lattice data [2–5] as well as hard-wall and soft-wall models. It is found that the hard-wall model cannot produce Regge spectra, and the soft-wall model cannot simultaneously produce the correct Regge slope and the ground state of the scalar glueball. As was shown in Ref. [29], the Regge slope and the ground state of the scalar glueball can be correctly produced in the dynamical soft-wall holographic QCD model with only one parameter.

Table 3. The mass spectra of 0^{++} glueballs in the dynamical soft-wall model, compared with combined lattice data [2–5], and hard-wall model ($z_m = 452$ MeV), soft-wall model with SW† indicates μ_G is fixed by lowest mass of 0^{++} glueball, and SW‡ indicates μ_G is fixed by Regge slope of 0^{++} glueball. The unit is in MeV.

J^{PC}	Lattice	HW	SW†	SW‡	DSW
0^{++}	1475-1730	1730	1730	2828	1593
0^{*++}	2670-2830	3168	2119	3464	2618
0^{**++}	3370	4593	2447	4000	3311
0^{***++}	3990	6016	2735	4472	3877

With the parameter fixed by the scalar glueball, we calculate the vector and tensor glueball masses in the dynamical soft-wall model and compare with lattice data as well as results from hard-wall and soft-wall models. The results are shown in Table 4. It is observed that for vector and tensor glueballs, the results from the dynamical holographic QCD model are far away from lattice data. Especially, the masses for higher spin states are too heavy compared with lattice data. The glueball masses from the hard-wall model are in general lighter than the lattice results. Among the three models, the soft-wall model (SW‡) with the parameter fixed by the Regge slope can produce reasonably good results compared with lattice data. However, none of the models can distinguish even and odd parity states for glueballs with the same spin.

Table 4. The mass spectra of vector and tensor glueballs in the dynamical soft-wall model, compared with lattice data, and hard-wall model ($z_m = 452$ MeV), soft-wall model with SW† indicates μ_G is fixed by lowest mass of 0^{++} glueball, and SW‡ indicates μ_G is fixed by Regge slope of 0^{++} glueball. The unit is in MeV.

J^{PC}	Lattice	HW1	SW†	SW‡	DSW
0^{-+}	2590	1730	1730	2828	1593
0^{*-+}	3640	3168	2119	3464	2618
0^{--}	5166	3658	2447	4000	10759
1^{+-}	2940	2571	1934	3162	7535
1^{--}	3850	2571	1934	3162	7535
2^{++}	2400	2134	1901	3108	4328
2^{-+}	3100	2134	1901	3108	4328
2^{*-+}	3890	3646	2260	3696	5233
2^{+-}	4140	2927	2201	3598	7830
2^{--}	3930	2927	2201	3598	7830

In the next section, we will improve the dynamical soft-wall holographic QCD model in order to produce reasonable glueball spectra.

5 Glueball spectra in modified dynamical soft-wall holographic QCD model

We observed from the last section that the masses for higher spin glueballs are too heavy compared with lattice data, while these states are reasonable in the soft-wall model. This indicates that only scalar glueballs are sensitive to the deformed metric, and other glueballs are not excited from this deformed metric background. Therefore we introduce a deformed 5D mass squared for glueballs. In order to distinguish even and odd parity, we introduce a positive and negative coupling between the dilaton field and glueballs, respectively. With this setup, now the 5D action for the scalar, vector and tensor glueballs $\mathscr{G}(x,z)$ take the following form:

$$S_{\mathscr{G}} = -\frac{1}{2}\int \mathrm{d}^5x\sqrt{g_s}\mathrm{e}^{-p\Phi}(\partial_M\mathscr{G}\partial^M\mathscr{G} + M^2_{\mathscr{G},5}(z)\mathscr{G}^2) \quad (40)$$

$$S_V = -\frac{1}{2}\int \mathrm{d}^5x\sqrt{g_s}\mathrm{e}^{-p\Phi}\left(\frac{1}{2}F^{MN}F_{MN} + M^2_{\mathscr{V},5}(z)\mathscr{V}^2\right), \quad (41)$$

$$\begin{aligned} S_T = -\frac{1}{2}\int \mathrm{d}^5x\sqrt{g_s}\mathrm{e}^{-p\Phi}&(\nabla_L h_{MN}\nabla^L h^{MN} \\ &-2\nabla_L h^{LM}\nabla^N h_{NM} + 2\nabla_M h^{MN}\nabla_N h \\ &-\nabla_M h\nabla^M h + M^2_{h,5}(z)(h^{MN}h_{MN} - h^2)), \end{aligned} \quad (42)$$

where $M_5^2(z) = M_5^2\mathrm{e}^{-2\Phi/3}$, $p = 1$ for even parity and $p = -1$ for odd parity.

The equation of motion for any glueball $\mathscr{A}$ can be brought into the Schroedinger-like equation

$$-\mathscr{A}_n^{''} + V_{\mathscr{A}}\mathscr{A}_n = m^2_{\mathscr{A},n}\mathscr{A}_n, \quad (43)$$

with the 5D effective Schroedinger potential

$$V_{\mathscr{A}} = \frac{cA_s^{''} - p\Phi^{''}}{2} + \frac{(cA_s^{'} - p\Phi^{'})^2}{4} + \mathrm{e}^{2A_s - \frac{2}{3}\Phi}M^2_{\mathscr{A},5}, \quad (44)$$

where $c = 1$ for the 1-form and $c = 3$ for the 0-form and 2-form, and $M^2_{\mathscr{A},5}$ is the value given in Table 1.

In order to distinguish glueballs with the same value of M_5^2 but different parity, such as the 0^{++} and 0^{-+} glueballs, we have introduced the positive and negative

coupling between the dilaton field and glueballs, respectively. The negative dilaton [37, 38] and positive dilaton [18] have been further discussed in detail in [39–43]. From Eq.(46), we can see that in the dynamical soft-wall model, the positive and negative coupling between the dilaton field and glueballs only induces an effective potential difference:

$$\Delta V_{\mathscr{A}} = \Phi^{''} + c\Phi^{'} A_s^{'}. \tag{45}$$

It was pointed in Ref. [41] that a negative dilaton coupling is equivalent to adding an effective potential

$$\Delta \mathcal{L}_{\mathscr{A}} = \mathrm{e}^{-2A_s}(\Phi^{''} + c\Phi^{'} A_s^{'}) \tag{46}$$

in the Lagrangian of positive dilaton coupling in Eq. (42). Therefore, the spectra of different parity glueballs are split, and the Regge slopes depending on μ are equal.

Comparing the 5D effective Schroedinger potential Eq. (46) with Eqs. (27), (31) and (36), we can see the effect of the deformed 5D mass square $M_5^2(z) = M_5^2\mathrm{e}^{-2\Phi/3}$ is to counteract the deform metric background. In Fig. 1 and Fig. 2, we show the 5D effective Schroedinger potential Eq. (46) as a function of z and compare with results from the soft-wall model and the original dynamical soft-wall model. It is found that at infrared (IR) scale, except for the scalar glueball 0^{++}, the 5D effective Schroedinger potential for

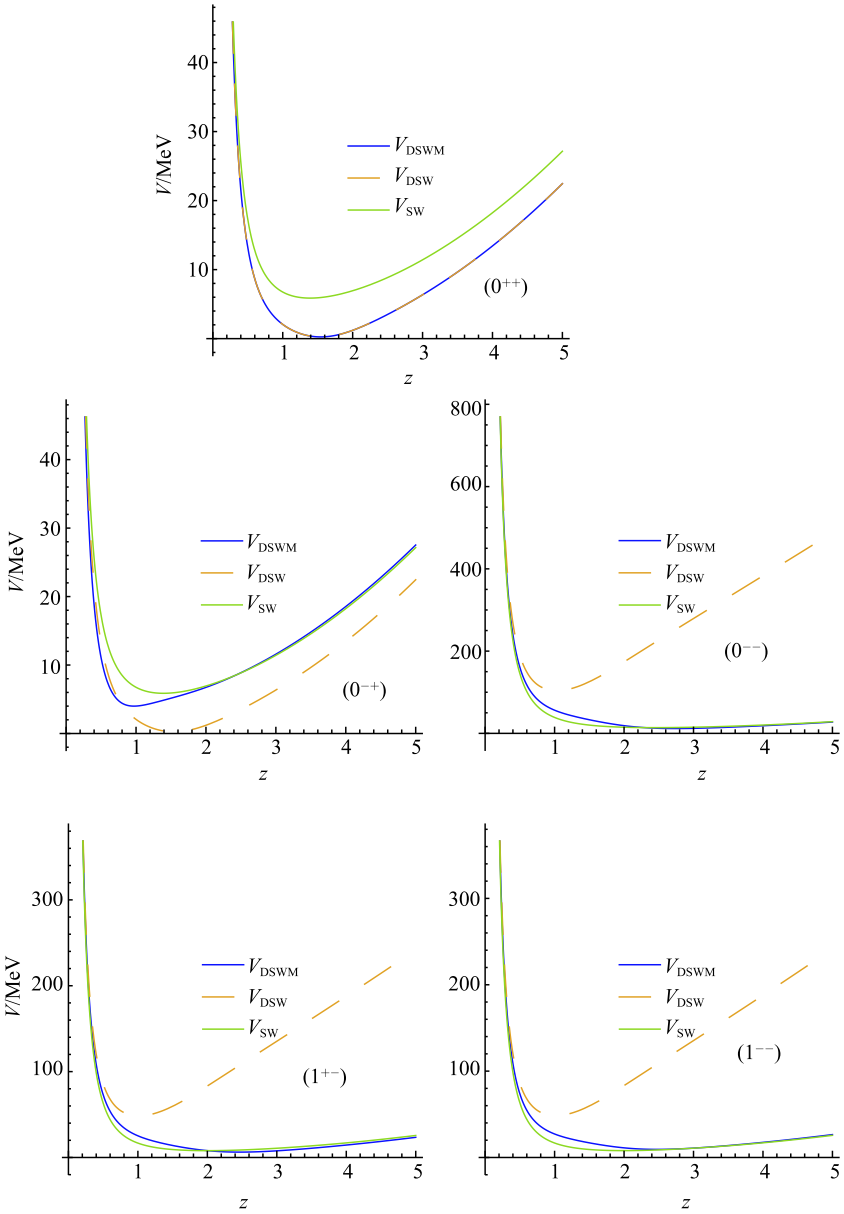

Fig. 1. (color online) The effective Schroedinger potential V of scalar and vector glueballs in the soft-wall model (green thick line), dynamical soft-wall model (orange dashed line) and dynamical soft-wall model with modified M_5^2(blue line).

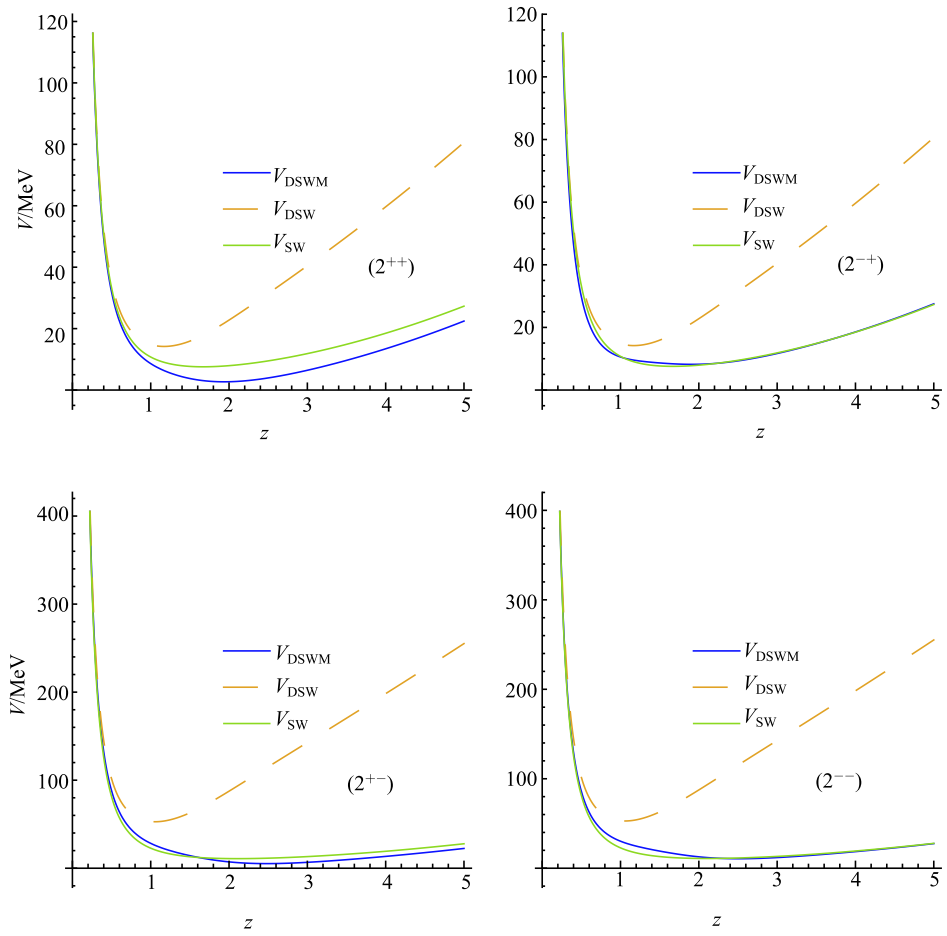

Fig. 2. (color online) The effective Schroedinger potential V of tensor glueballs in the soft-wall model (green thick line), dynamical soft-wall model (orange dashed line) and dynamical soft-wall model with modified M_5^2 (blue line).

other glueballs in the modified dynamical soft-wall holographic QCD model coincides with those from the soft-wall model. The parity difference $p = \pm$ only changes the 5D effective Schroedinger potential in the range $0.5 < z < 2$.

The final results of the glueball spectra in the modified dynamical holographic QCD model are shown in Fig. 3 and in Table 5 with details. It is found that with only one parameter $\mu_G = 1$GeV, which is fixed by the Regge slope of the scalar glueball spectra, one can produce almost all glueball spectra in good agreement with lattice data, except for three trigluon glueball states 0^{--}, 0^{+-} and 2^{+-}, whose masses are 1.5 GeV lighter than lattice results. Considering that we only take the simplest quadratic dilaton profile, which corresponds to dimension-2 gluon condensate (or effectively two-gluon condensate) in the vacuum, our results might indicate that these three trigluon glueballs 0^{--}, 0^{+-} and 2^{+-} are dominated by the three-gluon condensate contribution. It is worth mentioning that by introducing the positive and negative coupling between the dilaton field and glueballs, we can distinguish glueballs with the same value of M_5^2 but different parity, such as the 0^{++} and 0^{-+} glueballs. Surprisingly, from Table 5, we can see that without introducing any extra parameter, the mass differences for 0^{++} and 0^{-+} and their excitations as well as for other parity partners are in good agreement with lattice results. This indicates that it is practical to relate the positive and negative coupling between the dilaton field and glueballs to the parity of hadron spectra.

6 Conclusion and discussion

In this work, we have studied scalar, vector and tensor glueball spectra in the framework of a 5-dimension dynamical holographic QCD model, where the metric structure is deformed self-consistently by the dilaton field. It is found that only scalar glueballs are excited from this deformed metric background, and other glueballs excited from this deformed metric background are much heavier than lattice data. Therefore, for higher spin glueballs, we introduce a deformed 5-dimension mass in order to

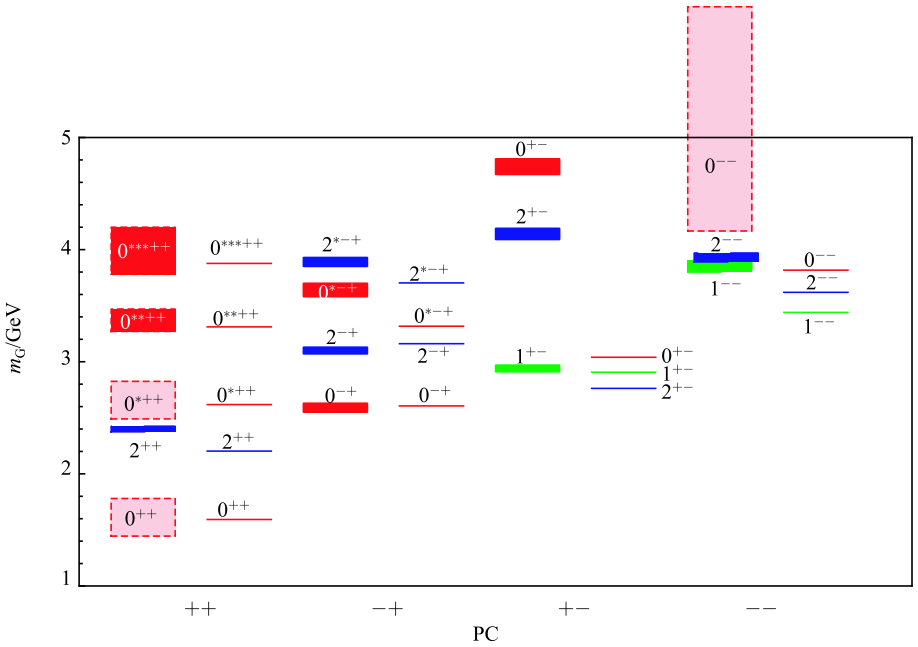

Fig. 3. (color online) The mass spectra of glueballs in the modified dynamical soft-wall model with $\mu = 1$ GeV (line) compared with the lattice result [2–6] (rectangle).

Table 5. The mass of glueball spectra in Lattice QCD [2–6], Flux tube model [7], QCDSR [9, 10, 35, 44–46] and modified dynamical soft-wall model. Note that 0^{++}§ is trigluonium. The unit is in GeV.

J^{PC}	LQCD	flux tube model	QCDSR	MDSM
0^{++}	1.475–1.73	1.52	1.5	1.593
0^{*++}	2.67–2.83	2.75	–	2.618
0^{**++}	3.37	–	–	3.311
0^{***++}	3.99	–	–	3.877
0^{-+}	2.59	2.79	2.05	2.606
0^{*-+}	3.64	–	–	3.317
0^{--}	5.166	2.79	3.81	3.817
0^{+-}	4.74	2.79	4.57	3.04
0^{++}§	–	–	3.1	2.667
1^{+-}	2.94	2.25	–	2.954
1^{--}	3.85	–	–	3.44
2^{++}	2.4	2.84	2	2.203
2^{-+}	3.1	2.84	–	3.161
2^{*-+}	3.89	–	–	3.703
2^{+-}	4.14	2.84	6.06	2.786
2^{--}	3.93	2.84	–	3.619

counteract the effect of the deformed metric background. In order to distinguish glueballs with even and odd parities, we introduce the positive and negative coupling between the dilaton field and glueballs.

With these set-ups, we calculated the glueball spectra with only one free parameter in the dynamical holographic QCD model, which is fixed by the scalar glueball spectra. It is found that all two-gluon glueball spectra produced in the dynamical holographic QCD model are in good agreement with lattice data. We investigated six trigluon glueballs. Among these trigluon glueballs, the produced masses for $1^{\pm-}$ and 2^{--} are in good agreement with lattice data, and the produced masses for 0^{--}, 0^{+-} and 2^{+-} are around 1.5 GeV lighter than lattice results. Considering that we only take the simplest quadratic dilaton profile, which corresponds to dimension-2 gluon condensate (or effectively two-gluon condensate) in the vacuum, our results might indicate that the three trigluon glueballs 0^{--}, 0^{+-} and 2^{+-} are dominated by three-gluon condensate contribution. Further studies with a more complicated dilaton profile are needed.

References

1 M. Gell-Mann, Acta Phys. Austriaca Suppl., **9**: 733 (1972)
2 C. J. Morningstar and M. J. Peardon, Phys. Rev. D, **60**: 034509 (1999) [hep-lat/9901004]
3 B. Lucini and M. Teper, JHEP, **0106**, 050 (2001) [hep-lat/0103027]
4 H. B. Meyer, arxiv: hep-lat/0508002
5 Y. Chen, A. Alexandru, S. J. Dong, T. Draper, I. Horvath, F. X. Lee, K. F. Liu and N. Mathur *et al*, Phys. Rev. D, **73**: 014516 (2006) [hep-lat/0510074]
6 E. Gregory, A. Irving, B. Lucini, C. McNeile, A. Rago, C. Richards and E. Rinaldi, JHEP, **1210**: 170 (2012) [arXiv:1208.1858 [hep-lat]]
7 N. Isgur and J. E. Paton, Phys. Rev. D, **31**: 2910 (1985)

8 T. Huang, H. Y. Jin and A. L. Zhang, Phys. Rev. D, **59**: 034026 (1999) [hep-ph/9807391]
9 C. -F. Qiao and L. Tang, Phys. Rev. Lett., **113**: 221601 (2014)
10 C. F. Qiao and L. Tang, arXiv:1509.00305 [hep-ph]
11 V. Mathieu, N. Kochelev and V. Vento, arXiv:0810.4453 [hep-ph]; E. Klempt and A. Zaitsev, Phys. Rept., **454**: 1 (2007); C. Amsler and N. A. Tornqvist, Phys. Rept., **389**: 61 (2004)
12 J. M. Maldacena, Adv. Theor. Math. Phys., **2**: 231 (1998) [hep-th/9711200]
13 S. S. Gubser, I. R. Klebanov and A. M. Polyakov, Phys. Lett. B, **428**: 105 (1998) [hep-th/9802109]
14 E. Witten, Adv. Theor. Math. Phys., **2**: 253 (1998) [hep-th/9802150]
15 O. Aharony, S. S. Gubser, J. Maldacena, H. Ooguri, Y. Oz, Phys. Rept., **323** 183 (2000); O. Aharony, arXiv:hep-th/0212193; A. Zaffaroni, PoS **RTN2005**, 005 (2005); J. Erdmenger, N. Evans, I. Kirsch and E. Threlfall, Eur. Phys. J. A, **35**: 81 (2008), [arXiv:0711.4467 [hep-th]]
16 P. Kovtun, D. T. Son and A. O. Starinets, Phys. Rev. Lett., **94**: 111601 (2005) [arXiv:hep-th/0405231]
17 J. Erlich, E. Katz, D. T. Son and M. A. Stephanov, Phys. Rev. Lett., **95**: 261602 (2005)
18 A. Karch, E. Katz, D. T. Son and M. A. Stephanov, Phys. Rev. D, **74**: 015005 (2006)
19 T. Sakai and S. Sugimoto, Prog. Theor. Phys., **113**: 843 (2005); Prog. Theor. Phys., **114**: 1083 (2006); G. F. de Teramond and S. J. Brodsky, Phys. Rev. Lett., **94**: 201601 (2005); L. Da Rold and A. Pomarol, Nucl. Phys. B, **721**: 79 (2005); K. Ghoroku, N. Maru, M. Tachibana and M. Yahiro, Phys. Lett. B, **633**: 602 (2006); O. Andreev, V. I. Zakharov, arXiv:hep-ph/0703010; Phys. Rev. D, **74**: 025023 (2006); M. Kruczenski, L. A. P. Zayas, J. Sonnenschein and D. Vaman, JHEP, **06**: 046 (2005); S. Kuperstein and J. Sonnenschein, JHEP, **11**: 026 (2004); H. Forkel, M. Beyer and T. Frederico, JHEP, **0707**: 077 (2007)
20 Deog Ki Hong, Takeo Inami, and Ho-Ung Yee, Phys. Lett. B, **646**:165-171 (2007); Kanabu Nawa, Hideo Suganuma, and Toru Kojo, Phys.Rev.D **75**: 086003 (2007); Deog Ki Hong, Mannque Rho, Ho-Ung Yee, and Piljin Yi, Phys.Rev.D **76**: 061901 (2007)
21 C. Csaki, H. Ooguri, Y. Oz and J. Terning, JHEP, **9901**: 017 (1999); R. de Mello Koch, A. Jevicki, M. Mihailescu and J. P. Nunes, Phys. Rev. D, **58**: 105009 (1998); M. Zyskin, Phys. Lett. B, **439**: 373 (1998) ; J. A. Minahan, JHEP, **9901**: 020 (1999); C. Csaki, Y. Oz, J. Russo and J. Terning, Phys. Rev. D, **59**: 065012 (1999); R. Apreda, D. E. Crooks, N. J. Evans and M. Petrini, JHEP, **0405**: 065 (2004)
22 R. C. Brower, S. D. Mathur and C. I. Tan, Nucl. Phys. B, **587**: 249 (2000)
23 H. Boschi-Filho and N. R. F. Braga, JHEP, **0305**: 009 (2003); H. Boschi-Filho and N. R. F. Braga, Eur. Phys. J. C, **32**: 529 (2004); H. Boschi-Filho, N. R. F. Braga and H. L. Carrion, Phys. Rev. D, **73**: 047901 (2006)
24 P. Colangelo, F. De Fazio, F. Jugeau and S. Nicotri, Phys. Lett. B, **652**: 73 (2007) [hep-ph/0703316]. L. Bellantuono, P. Colangelo and F. Giannuzzi, arXiv:1507.07768 [hep-ph]
25 H. Forkel, Phys. Rev. D, **78**: 025001 (2008) [arXiv:0711.1179 [hep-ph]]
26 T. Sakai and S. Sugimoto, Prog. Theor. Phys., **113**: 843 (2005); Prog. Theor. Phys., **114**, 1083 (2006)
27 K. Hashimoto, C. I. Tan and S. Terashima, Phys. Rev. D, **77**: 086001 (2008) [arXiv:0709.2208 [hep-th]]. F. Brünner, D. Parganlija and A. Rebhan, Phys. Rev. D, **91** (10): 106002 (2015) [arXiv:1501.07906 [hep-ph]]. F. Brünner and A. Rebhan, Phys. Rev. Lett., **115** (13): 131601 (2015) [arXiv:1504.05815 [hep-ph]]
28 D. Li, M. Huang and Q. -S. Yan, Eur. Phys. J. C, **73**: 2615 (2013) [arXiv:1206.2824 [hep-th]]
29 D. Li and M. Huang, JHEP, **1311**: 088 (2013) [arXiv:1303.6929 [hep-ph]]
30 D. Li and M. Huang, arXiv:1311.0593 [hep-ph]
31 D. Li, J. Liao and M. Huang, Phys. Rev. D, **89** (12): 126006 (2014) [arXiv:1401.2035 [hep-ph]]
32 D. Li, S. He and M. Huang, JHEP, **1506**: 046 (2015) [arXiv:1411.5332 [hep-ph]]
42 K. Chelabi, Z. Fang, M. Huang, D. Li and Y. L. Wu, arXiv:1511.02721 [hep-ph]
34 Jaffe R. L., Phys. Rev. D, **15**: 267 (1977)
35 K. F. Liu, Prog. Theor. Phys. Suppl., **168**: 160 (2007); Liu K. F., Wong C. W., Phys. Lett. B, **107**: 391 (1981); Cheng H. Y., Chua C. K., Liu K. F., Phys. Rev. D, **74**: 094005 (2006); 't Hooft G., Isidori G., et al, Phys. Lett. B, **662**: 424 (2008); Zhao Q., Zou B. s., Ma Z. b., Phys. Lett. B, **631**: 22 (2005); Bugg D. V., Peardon M. J., Zou B. S., Phys. Lett. B, **486** (2000): 49; Narison S., Nucl.Phys.Proc.Suppl., **186**:306-311 (2009)
36 B. A. Li, Phys. Rev. D, **81**: 114002 (2010) [arXiv:0912.2323 [hep-ph]]. H. Y. Cheng, AIP Conf. Proc., **1257**, 477 (2010) [arXiv:0912.3561 [hep-ph]]. S. Janowski, F. Giacosa and D. H. Rischke, Phys. Rev. D, **90** (11): 114005 (2014) [arXiv:1408.4921 [hep-ph]]. W. I. Eshraim, arXiv:1509.09117 [hep-ph]. S. He, M. Huang and Q. S. Yan, Phys. Rev. D, **81**: 014003 (2010) [arXiv:0903.5032 [hep-ph]]. T. K. Mukherjee, M. Huang and Q. S. Yan, Phys. Rev. D, **86**: 114022 (2012) [arXiv:1203.5717 [hep-ph]]. T. K. Mukherjee and M. Huang, Phys. Rev. D, **89** (7): 076002 (2014) [arXiv:1311.1313 [hep-ph]]
37 F. Zuo, Phys. Rev. D, **82**: 086011 (2010) doi:10.1103/PhysRevD.82.086011 [arXiv:0909.4240 [hep-ph]]
38 S. J. Brodsky, G. F. de Teramond and A. Deur, Phys. Rev. D, **81**: 096010 (2010) doi:10.1103/PhysRevD.81.096010 [arXiv:1002.3948 [hep-ph]]
39 A. Karch, E. Katz, D. T. Son and M. A. Stephanov, JHEP, **1104**: 066 (2011) doi:10.1007/JHEP04(2011)066 [arXiv:1012.4813 [hep-ph]]
40 D. Li, S. He, M. Huang and Q. S. Yan, JHEP, **1109**: 041 (2011) doi:10.1007/JHEP09(2011)041 [arXiv:1103.5389 [hep-th]]
41 T. Gutsche, V. E. Lyubovitskij, I. Schmidt and A. Vega, Phys. Rev. D, **85**: 076003 (2012) doi:10.1103/PhysRevD.85.076003 [arXiv:1108.0346 [hep-ph]]
42 K. Chelabi, Z. Fang, M. Huang, D. Li and Y. L. Wu, Phys. Rev. D, **93** (10): 101901 (2016) doi:10.1103/PhysRevD.93.101901 [arXiv:1511.02721 [hep-ph]]
43 K. Chelabi, Z. Fang, M. Huang, D. Li and Y. L. Wu, JHEP, **1604**: 036 (2016) doi:10.1007/JHEP04(2016)036 [arXiv:1512.06493 [hep-ph]]
44 S. Narison and G. Veneziano, Int. J. Mod. Phys. A, **4**: 2751 (1989). doi:10.1142/S0217751X89001060
45 J. I. Latorre, S. Narison and S. Paban, Phys. Lett. B, **191**: 437 (1987). doi:10.1016/0370-2693(87)90636-8
46 S. Narison, Nucl. Phys. B, **509**: 312 (1998) doi:10.1016/S0550-3213(97)00562-2 [hep-ph/9612457]